Lipidomics suggests a new role for ceramide synthase in phagocytosis

Divya Pathak[1,3], Neelay Mehendale[2,3], Shubham Singh[2], Roop Mallik[1], Siddhesh S. Kamat[2,*].

[1]Department of Biological Sciences, Tata Institute of Fundamental Research, Homi Bhabha Road, Mumbai, 400005, India

[2]Department of Biology, Indian Institute of Science Education and Research, Dr. Homi Bhabha Road, Pashan, Pune 411008, India.

[3]These authors contributed equally to the work.

*To whom the correspondence should be made: siddhesh@iiserpune.ac.in

Supplementary Information

Table of contents

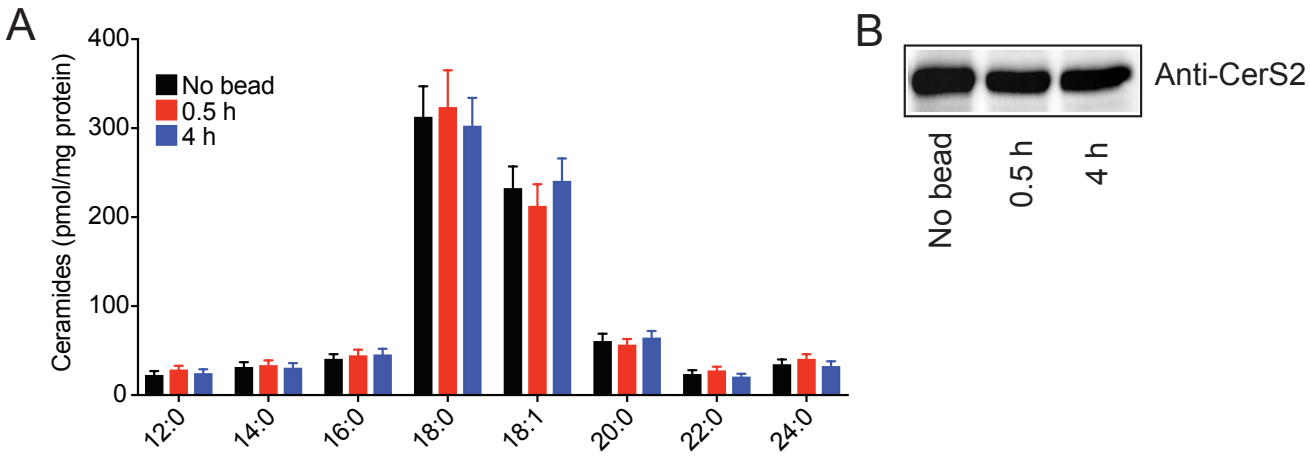

Supplementary Figure 1. Cellular concentration of ceramides and CerS2 following bead phagocytosis from RAW264.7 cells. As a control experiment to determine whether (**A**) cellular ceramides and (**B**) cellular CerS2 were altered in RAW264.7 cells when fed with beads, and concentrations of ceramides and CerS2 were measured by LC-MS/MS and western blot analysis respectively at 0.5 and 4 h post bead feeding (which represent time points of EP and LP maturation respectively). Based on these data, both these cellular levels are unaltered, suggesting that changes in ceramides and CerS2 are indeed EP and LP specific. The data in panel (**A**) represents mean ± s. e. m. for 4 biological replicates, while the data in panel (**B**) was performed in duplicate with reproducible results.

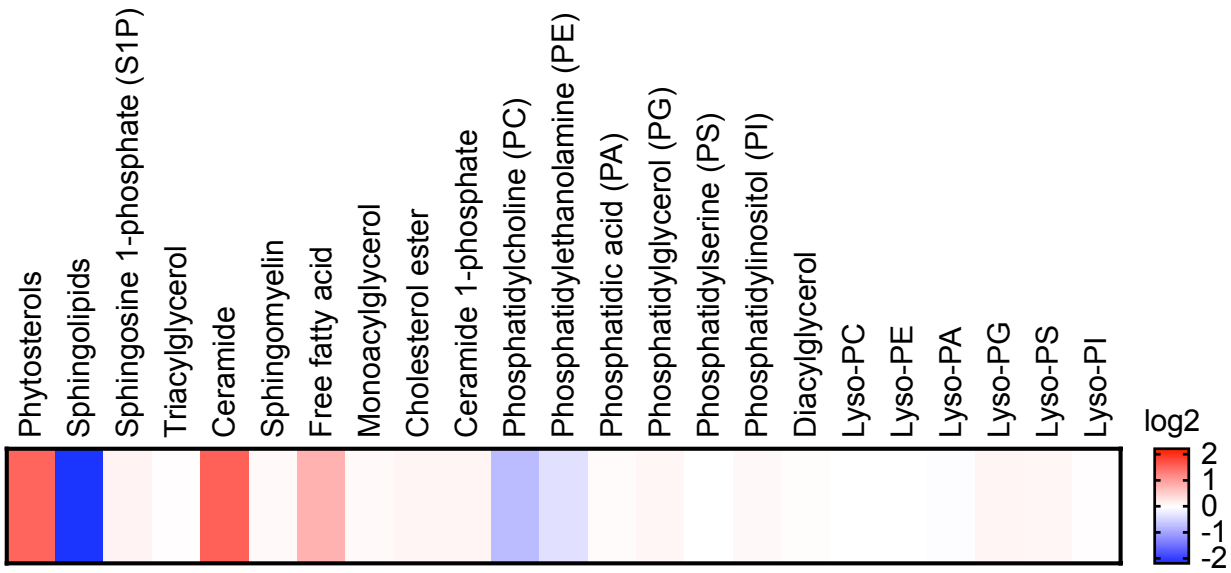

Supplementary Figure 2. **Lipidomic characterization of EPs and LPs from *Dictyostelium discoideum*.** Heat map plot showing the different lipid classes assessed by LC-MS/MS analysis for EPs and LPs from *Dictyostelium discoideum*. The heat map plot represents an average of fold changes (LP/EP) on a log2 scale for different lipids from a particular lipid class. Blue and red color changes show enrichment of a particular lipid class on EP and LP respectively. Data represents 6 biological replicates per group. See **Supplementary Table 1** for complete datasets.

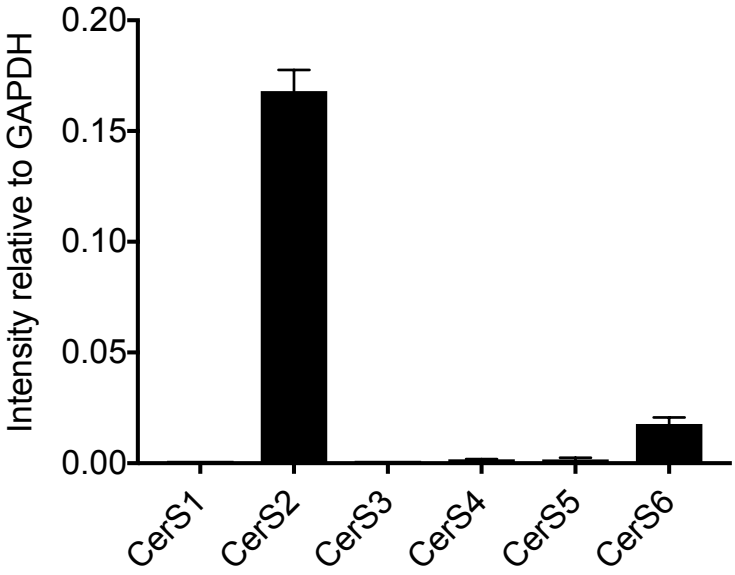

Supplementary Figure 3. **Expression profile for different ceramide synthase isoforms in RAW264.7 mouse macrophages**. The mRNA levels of ceramide synthase isoforms 1 – 6 in mammalian RAW264.7 cells relative to GAPDH from public large-scale gene expression studies (http://biogps.org/)[1, 2]. The mRNA expression data suggests that CerS2 is the major ceramide synthase in RAW264.7 mouse macrophages[3], with probably some contribution from CerS6. Data represents mean ± s. d. for 2 biological replicates.

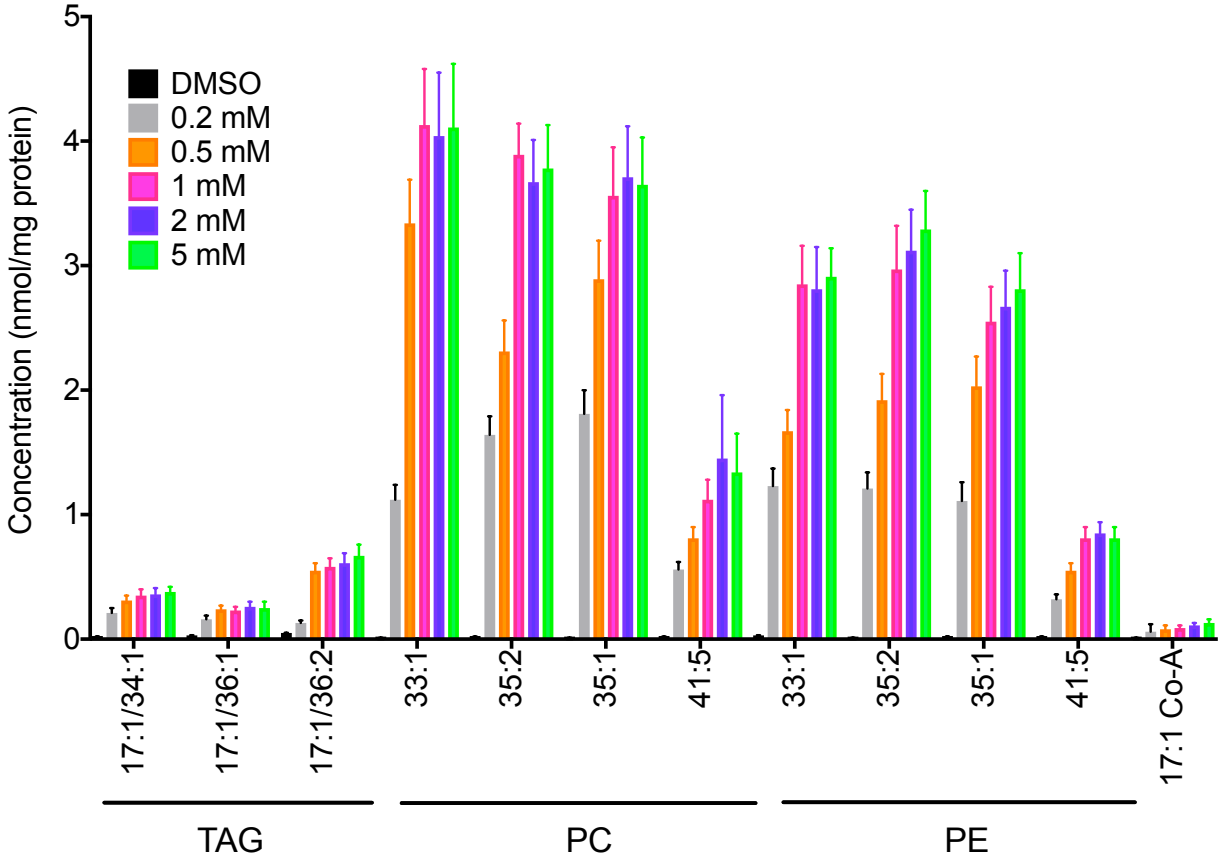

Supplementary Figure 4. Incorporation of C17:1 FFA into cellular phospholipids. Concentrations of C17:1-containing storage lipids, namely triglycerides (TAG), phosphatidylcholines (PC), phosphatidylethanolamines (PE) and co-enzyme A (Co-A) from RAW264.7 mouse macrophages, following feeding varied concentrations of C17:1 FFA (0 – 5 mM, 4 h). Data shows that the C17:1 FFA is predominantly incorporated into cellular PC and PE lipids. Data represents mean ± s. e. m. for 4 biological replicates per group. Since there was no significant change beyond feeding 1 mM C17:1 FFA, hence this concentration was chosen for the feeding experiments.

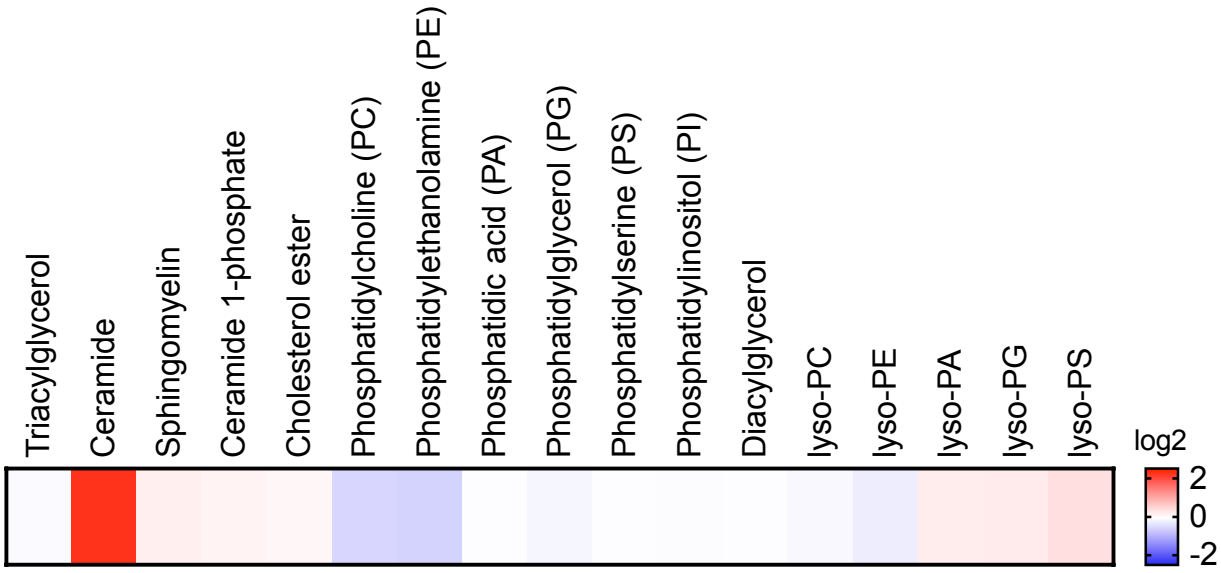

Supplementary Figure 5. Lipidomics characterization of heptadecenoic acid (C17:1)-containing lipids in EPs and LPs following C17:1 FFA feeding to RAW264.7 mouse macrophages. Heat map plot showing the different lipid classes containing C17:1 assessed by comparative LC-MS/MS analysis for EPs and LPs from RAW264.7 cells fed with C17:1 FFA (1 mM, 4 h), prior to phagocytosis. The heat map plot represents the ratio of the mean value for LPs divided by the mean value for EPs for a particular lipid on a log2 scale. Blue and red color changes show enrichment of a lipid class on EPs and LPs respectively. Data represents mean of 4 biological replicates per group. See **Supplementary Table 1** for complete dataset.

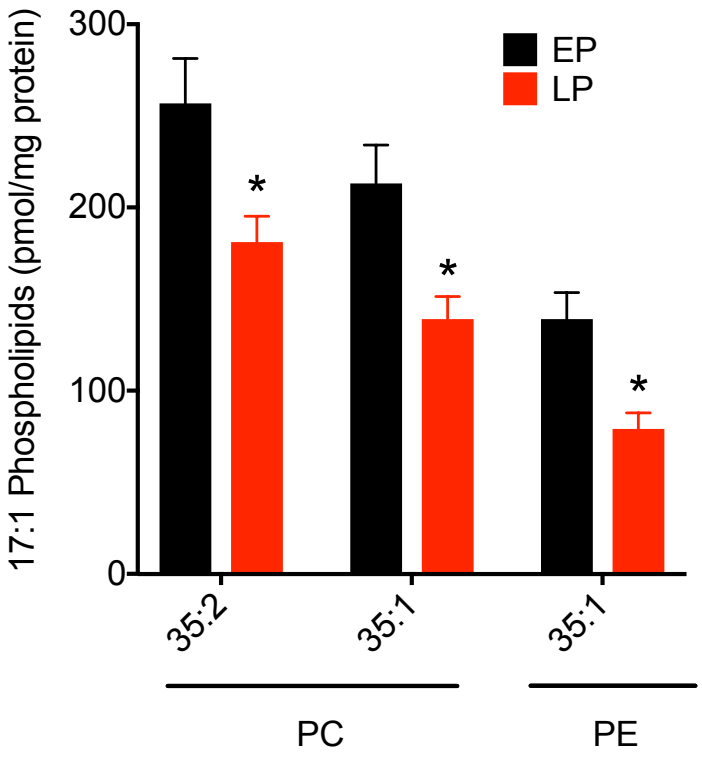

Supplementary Figure 6. Phospholipid concentrations of EPs and LPs following C17:1 FFA feeding to RAW264.7 mouse macrophages. Quantitative lipidomics measurements of C17:1-containing PC and PE lipids showing changes in absolute levels between EPs and LPs groups. Data represents mean ± s. e. m. for 4 biological replicates. * $P < 0.05$ by Student's t-test for EP versus LP preparations. See **Supplementary Table 1** for complete dataset.

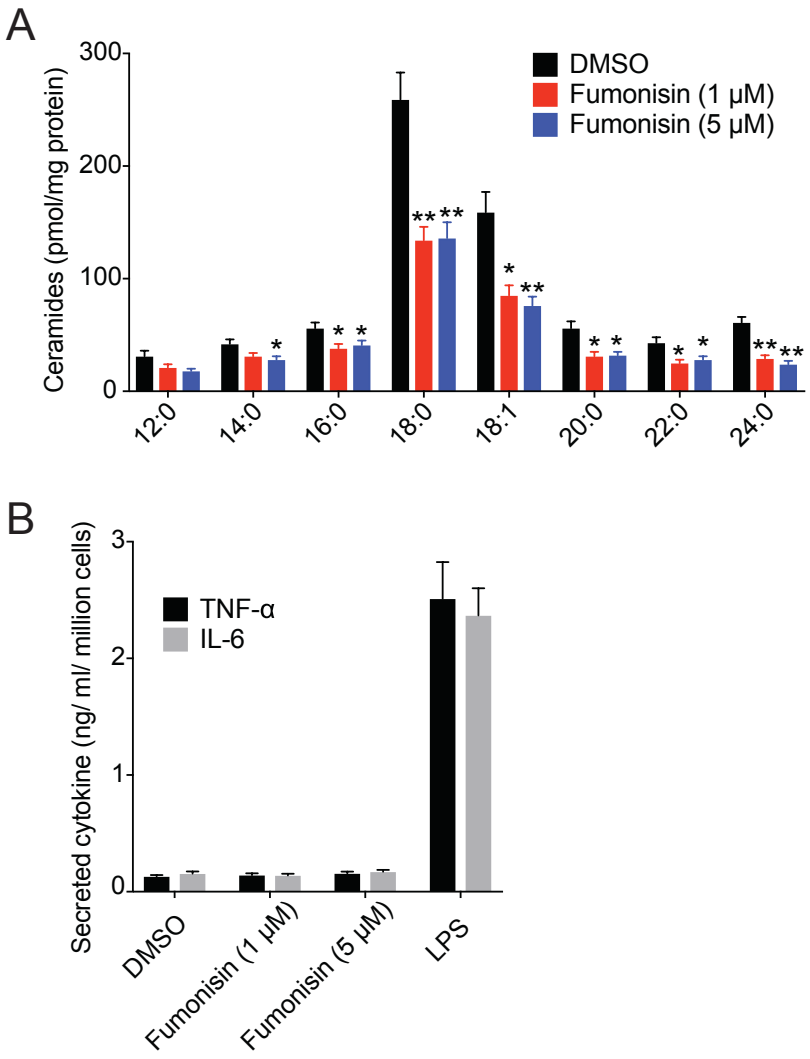

Supplementary Figure 7. Pharmacological blockade of CerS2 by fumonisin in RAW264.7 mouse macrophages. (**A**) Ceramide concentrations of RAW264.7 cells following treatment with fumonisin (1 or 5 μM) or DMSO (control) for 4 h. Data represent mean ± s. e. m. for 4 biological replicates per group. * $P < 0.05$ and ** $P < 0.01$ by Student's t-test for treatment groups versus DMSO control. (**B**) Pro-inflammatory cytokine concentrations (TNF-α and IL-6) following treatment with fumonisin (1 or 5 μM) or DMSO (vehicle, negative control) or lipopolysaccharide (LPS, 10 μg mL^{-1}, positive control) for 4 h. Data represents mean ± s. e. m. for 8 biological replicates per group.

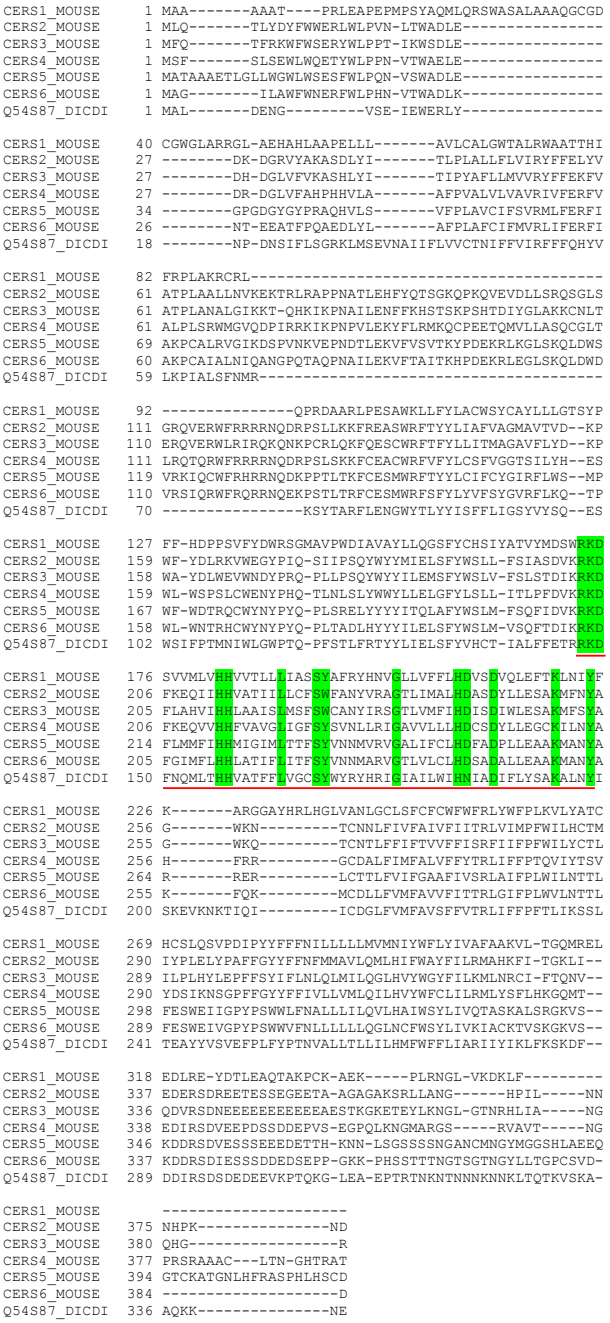

Supplementary Figure 8. Sequence alignment of mammalian (mouse) ceramide synthase isoforms (CerS 1 – 6) with ceramide synthase from *Dictyostelium discoideum* (CrsA, Q54S87). The residues highlighted in green represent the invariant catalytically important residues, while the residues underlined in red constitute the highly conserved *Lag1P* motif of ceramide synthase enzymes[4, 5].

Supplementary Table 1: MRM transitions and complete lipidomics data.

- Tab 1 ('**MRM transitions**'): MRM transitions, and MS parameters for all lipids assessed in this study.

- Tab 2 ('**RAW cells EP and LP data**'): Complete lipidomics dataset (all identified and quantified lipids) for EPs and LPs from RAW264.7 mouse macrophages.

- Tab 3 ('**Dictyostelium EP and LP data**'): Complete lipidomics dataset (all identified and quantified lipids) for EPs and LPs from *Dictyostelium discoideum*.

- Tab 4 ('**RAW cells 17_1 feeding expt**'): Concentrations of C17:1-containing lipids from EPs and LPs from RAW264.7 mouse macrophages post-feeding 1 mM C17:1 FFA for 4 h.

- Tab 5 ('**CerS2 inhibition RAW cells**'): Concentrations of sphingolipids from EPs and LPs after treating RAW264.7 mouse macrophages with fumonisin (5 μM, 4 h).

References:

[1] Wu, C., Jin, X., Tsueng, G., Afrasiabi, C., and Su, A. I. (2016) BioGPS: building your own mash-up of gene annotations and expression profiles, *Nucleic Acids Res 44*, D313-316.

[2] Wu, C., Orozco, C., Boyer, J., Leglise, M., Goodale, J., Batalov, S., Hodge, C. L., Haase, J., Janes, J., Huss, J. W., 3rd, and Su, A. I. (2009) BioGPS: an extensible and customizable portal for querying and organizing gene annotation resources, *Genome Biol 10*, R130.

[3] Halasiddappa, L. M., Koefeler, H., Futerman, A. H., and Hermetter, A. (2013) Oxidized phospholipids induce ceramide accumulation in RAW 264.7 macrophages: role of ceramide synthases, *PLoS One 8*, e70002.

[4] Spassieva, S., Seo, J. G., Jiang, J. C., Bielawski, J., Alvarez-Vasquez, F., Jazwinski, S. M., Hannun, Y. A., and Obeid, L. M. (2006) Necessary role for the Lag1p motif in (dihydro)ceramide synthase activity, *J Biol Chem 281*, 33931-33938.

[5] Levy, M., and Futerman, A. H. (2010) Mammalian ceramide synthases, *IUBMB Life 62*, 347-356.